Modeling and numerical simulation of gain of Nd-doped fiber amplifier in 1. 7um~1. 8um

Hequn Zhou [1]

[1]Xidian University, Shaanxi, China

*Corresponding author: 20009101555@stu.xidian.edu.cn

Abstract: Fiber amplifier is an important piece of equipment to ensure the long-distance communication of optical fiber. The rare-earth ion-doped fiber amplifier is a hot issue studied in many articles. However, few articles investigate Neodymium-doped fiber amplifiers for 1.7μm optical signal amplification because of the low signal gain. Therefore, this paper establishes the system model of Neodymium ion to realize the optical signal amplification in the 1.7μm band. It establishes its mathematical model by using the equation of rate and power transmission equation and solves it numerically to realize the numerical simulation of Neodymium-doped fiber amplifier for 1.7μm optical signal amplification, and studies the simulation results, summarizes the amplifier properties, and fits the results to get the mathematical expressions. This paper finds that the plot of gain variation with fiber position contains a linear asymptote with a slope less than zero. The asymptote is related to the initial signal light and the optical power of the pump. Increasing the doping concentration will cause the optical signal to converge to this asymptote faster. The numerical fitting results in this paper can be applied to the estimation of gains as well as to generate insights into theoretical studies, such as considering the possibility of applying the Weber distribution commonly used for infinite optical communication in fiber models.

Keywords: Optical amplifiers, Neodymium-doped fiber amplifier, 1. 7 μm fiber amplifier.

1. Introduction

Fiber optic communication has high capacity, long transmission distance, and high immunity to electromagnetic interference [1]. It is widely used in many fields such as communication, medical, and military engineering [2-4], and fiber optic amplifiers are also used in laser generation and transmission processes. For long-distance transmission of laser signals, their power attenuation over long distances is a major problem in fiber optic communication. Current technology has been able to limit well the power attenuation of 1500 nm band laser in optical fiber [5], but the research in the 1700 nm ~ 1800 nm band is not yet mature, in the current mostly thulium-doped, bismuth means to design optical fiber ampler(OFA), but still have a high power attenuation. The band, however, has special spectral properties, and contains absorption peaks for a variety of organic substances [6], such as fat and collagen. It is located in the trough region between the two absorption peaks of water [7], which makes it useful for organic detection as well as in the field of bioimaging. This paper simulate and model the gain of a Neodymium-doped amplifier by means of Neodymium doping. In 2004 Agger Soren et al. developed a single frequency distributed feedback doped thulium dioxide laser with a wavelength of 1735 nm [8] with a pump light wavelength of 790 nm and a threshold power of 59 mW. Its pump light wavelength is 790 nm and the threshold power is 59 mW. In this experiment, thulium, a rare earth element, was used as the amplification medium, and since then, the development of thulium-doped fiber amplifiers has been growing rapidly. Quimby et al. at Worcester Polytechnic Institute, USA, achieved a mid-infrared laser output of 4. 5 μm from 2008-2013 [9,10]. In 2014, J. M. O. Daniel et al. at the University of Southampton, UK, fabricated thulium-doped fibers using a 1565 nm laser pumped by a fiber core, achieving continuous laser output in the tuning range of 1660 nm to 1820 nm. The following year, J. M. O Daniel et al. obtained another laser output based on thulium-doped fiber at 1726 nm with an output frequency of 12. 6 W and a slope efficiency of 63%[11]. In 2019, Zhang Y et al. from the National University of Defense Technology developed a 1. 7 μm band tunable random Raman fiber laser (RFL) [12], using 1550 nm amplified spontaneous emission (ASE) light pumped Raman fiber to obtain a wavelength. The laser output was obtained at a wavelength of

1715 nm with an output power of 14. 5 W and a spectral purity of 98%. A w-type thulium-doped fiber 1. 7 μm band femtosecond laser was proposed by CHEN et al. of Nanyang Technological University in 2020. It can obtain a stable pulse of 174 fs in the region of 1. 7 μm to 1. 8 μm with a pulse energy of up to 128 nJ[13]. In January 2021, CHEN et al. from South China Normal University used an intracavity bandpass filter to suppress the long-wave emission while compensating the dispersion by a high numerical aperture fiber to obtain a spectrum with a central wavelength of 1737 nm to 1754 nm. At the same time, they found that the bandwidth dissipative soliton (dissipative soliton) from 1737 nm to 1754 nm could be obtained by optimizing the cavity dispersion. This is the first step to realize the chirped pulse amplification system in the 1700 nm band [14]. In 2021 Grimes Andrew et al. used cascaded Raman fiber lasers [15], producing lasers with an output power of 104 w at around 1700 nm and spectral purity of more than 90% in both continuous wave and pulsed situations. In March 2022, Zhu Yi-Huai et al. proposed and realized an all-fiberized self-synchronized picosecond pulsed stochastic Raman laser [16], the first stochastic pulsed fiber laser operating at 1700 nm wavelength band. In summary, there are three main methods for making fiber amplifiers in the 1700nm~1800nm band as follows: thulium-doped fiber-based method, special ion-based doping method, and nonlinear effect-based method. This paper aims to solve the numerical simulation problem of an Nd-doped YAG ceramic material fiber amplifier in the 1700-1800nm band. Through simulation, this paper discusses the relationship between fiber amplifier gain and doping concentration, pump initial light power, fiber length, and signal initial light power. In addition, this paper investigates how to set the asymptote to get the highest power gain. In the future, fiber optic amplifiers with low attenuation and high gain will be used in communication, medical and military applications.

2. Experimental method

In order to study the gain of the Nd-doped fiber amplifier in the 1700-1800nm band as affected by fiber length, doping concentration, and signal power, the Nd-doped fiber amplifier model is established. The model is based on the Nd-ion energy level structure, the laser number rate equation system and the laser power propagation equation. And the numerical solution method of Runge-Kutta methods is used to solve the model. The method has the advantages of high computational accuracy, convergence, and no need to calculate higher-order derivatives. In building the model, the direction of light propagation along the fiber as the positive direction. To establish a one-dimensional coordinate system, set z is the position coordinates, set the starting point of light into the fiber as the origin; t is the time, unit seconds s, the time of the signal light into the fiber as the time zero point.

2.1 Energy levels modeling of Nd^{3+}

The electron arrangement of Neodymium is $1s^2 2s^2 2p^6 3s^2 3p^6 3d^{10} 4s^2 4p^6 4d^{10}$, Figure 1 shows the energy level structure of trivalent Neodymium ion (Nd^{3+}).

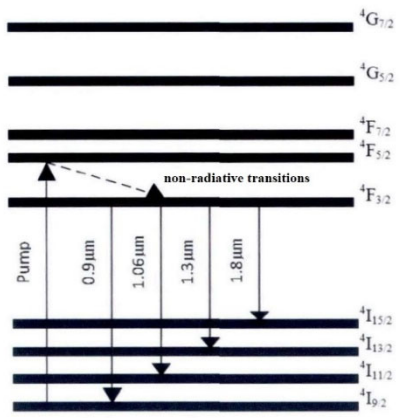


Figure 1. Structure of Nd^{3+} energy level[17]

Among them, $^4I_{9/2}$ is the ground state energy level of $\boldsymbol{Nd^{3+}}$, and the $\boldsymbol{Nd^{3+}}$ at this energy level will jump to $^4F_{3/2}$, $^4F_{5/2}$, $^4F_{7/2}$ and other excited energy levels under the excitation of pump light. Still, the $^4F_{5/2}$, $^4F_{7/2}$ energy levels are very short-lived and cannot form the particle number inversion [17]. The laser amplifier range studied in this experiment is from 1700 nm to 1800 nm. Peak number 1 from Figure 2(d) corresponds to the light released by the jump from $^4F_{3/2}$ to $^4I_{15/2}$, whose wavelength of 1739 nm is consistent with the spectral range studied in this paper, so the whole process can be regarded as a three-energy system containing $^4I_{9/2}$, $^4I_{15/2}$, and $^4F_{3/2}$.

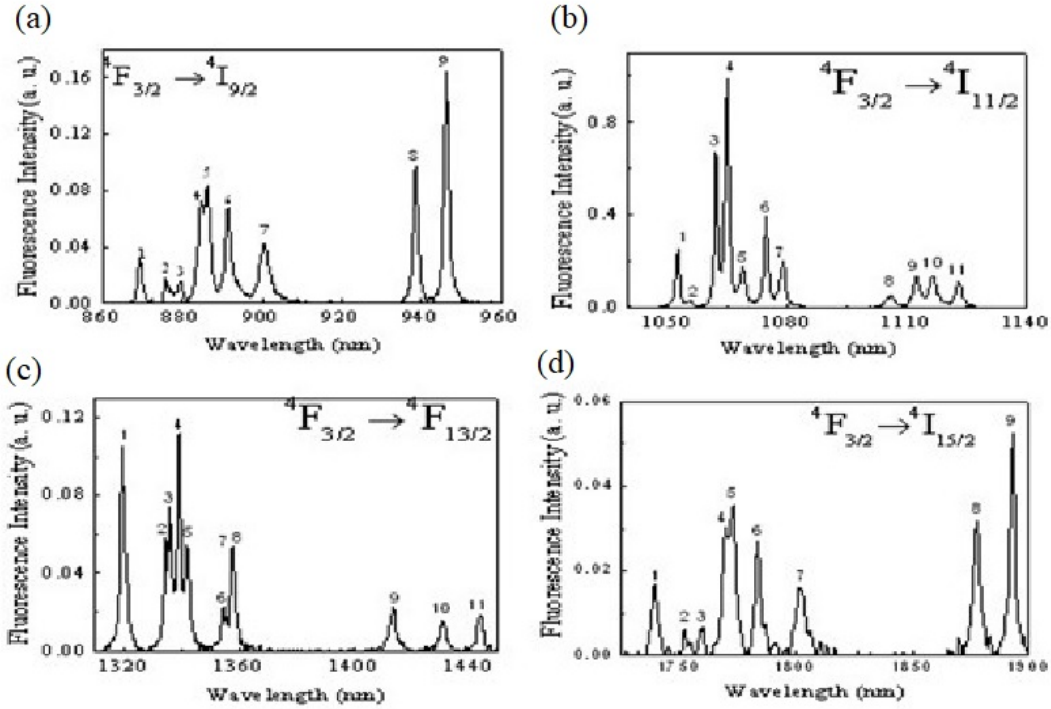


Figure 2. Fluorescence spectra for Nd^{3+}[18]

2.2 Rate equation of three energy levels system

For the three-energy level system, in order to calculate the bulk density of Neodymium ions at each energy level in the three-energy level structure of Neodymium in the fiber, the following rate equation can be established, where the corresponding parameters are shown in Table 1.

$$\frac{\partial N_1(z)}{\partial t} = -W_p(z) \times N_1(z) + A_{21} \times N_2(z) \tag{1}$$

$$\frac{\partial N_2(z)}{\partial t} = W_{32}(z) \times N_3(z) - W_{23}(z) \times N_2(z) - A_{21} \times N_2(z) + A_{32} \times N_3(z) \tag{2}$$

$$\frac{\partial N_3(z)}{\partial t} = W_p(z) \times N_1(z) + W_{23}(z) \times N_2(z) - W_{32}(z) \times N_3(z) - A_{32} \times N_3(z) \tag{3}$$

$$N = N_1(z) + N_2(z) + N_3(z) \tag{4}$$

Table.1. Table of parameters

Parameter	Physical Meaning	Values	Unit
N	Total $\boldsymbol{Nd^{3+}}$ bulk density	1.95×10^{24}	m^{-3}
A_{21}	Non-radiative jump rate of $^4I_{15/2}$ to $^4I_{9/2}$	1730[19]	s^{-1}
A_{32}	Non-radiative jump rate of $^4F_{3/2}$ to $^4I_{15/2}$	0[18]	s^{-1}
σ_{13}	Absorption cross section of $^4I_{9/2}$to $^4F_{3/2}$	5.6×10^{-24}[17]	m^2
σ_{23}	Absorption cross section of $^4I_{15/2}$ to $^4F_{3/2}$	3.6×10^{-24}	m^2
σ_{32}	$^4F_{3/2}$ to $^4I_{15/2}$emission cross-sectional area	3.6×10^{-24}[18]	m^2
ν_{13}	Absorbed photon frequency in $^4I_{9/2}$ to $^4F_{3/2}$	3.71×10^{14}[18]	s^{-1}
ν_{23}	Absorbed photon frequency in $^4I_{15/2}$to $^4F_{3/2}$	1.72×10^{14} [18]	s^{-1}
ν_{32}	Emitted photon frequency in $^4F_{3/2}$ to $^4I_{15/2}$	1.72×10^{14}	s^{-1}
$P_s(0)$	Signal light input power	10^{-6}	W
$P_p(0)$	Pump light input power	0. 1	W
α_p	Light material loss factor of pump light	0. 1	m^{-1}
α_s	Light material loss coefficient of signal light	0. 1	m^{-1}
$\Delta\nu$	Frequency half height full width	1150[18]	Hz
L	Fiber length	10	m
r	Fiber inner diameter	$2.5 \times 10^{-6} - 6$	m
λ_m	Central wavelength of $^4F_{3/2}$to $^4I_{15/2}$	1900[20]	Nm
N_1	The bulk density of Nd^{3+} at $^4I_{9/2}$		m^{-3}
N_2	The bulk density of Nd^{3+}at $^4I_{15/2}$		m^{-3}
N_3	The bulk density of Nd^{3+} at $^4IF_{3/2}$		m^{-3}
W_p	Pump light absorption rate		s^{-1}
W_{23}	Signal light absorption rate		s^{-1}
W_{32}	Signal Light Stimulated Emission Rate		s^{-1}
h	Planck constant		J·s
T	Ambient temperature		K
κ	Boltzmann constant		J/K
ε_0	Energy spacing between energy levels		J
G_1	Power Gain		100%
G_2	Logarithmic form of power gain		dB

In the three-energy level system of Nd^{3+}, equation (1) indicates that the ions at the $^4I_{9/2}$ energy levels are excited to other energy levels by the pump light, and the bulk density decreases. In contrast, the volume density of $^4I_{9/2}$ ions increases during the radiation-free jump to $^4I_{9/2}$ at the $^4I_{15/2}$ energy level. When the latter is smaller than the former, the volume density of ions at the $^4I_{9/2}$ energy level decreases, and the macroscopic manifestation is that ions at the $^4I_{9/2}$ energy level jumps to other energy levels. Equation (2) indicates that an ion at the $^4I_{15/2}$ energy level will receive an increase in its bulk density from ions excitedly emitted and radiolessly leapt by $^4F_{3/2}$, while it will decrease due to radioless leaps to $^4I_{9/2}$ and excited leaps to $^4F_{3/2}$. When the latter is smaller than the former, the volume density of $^4I_{15/2}$ energy level ions increases. The macroscopic manifestation is the jumping of other energy level ions to the $^4I_{15/2}$ energy level. Equation (3) represents the increase in bulk density of ions at $^4F_{3/2}$ due to the pumping leap of ions at $^4I_{9/2}$ in the presence of pump light and the excited leap of ions from $^4I_{15/2}$ in the presence of signal light. At the same time the bulk density decreases due to the excited radiative leap in the presence of signal light and the natural radiation-free leap to the $^4I_{15/2}$ energy level. When the latter value is smaller than the former, the number of $^4F_{3/2}$ ions decreases and the macroscopic manifestation is the leap

of $^4F_{3/2}$ ions to other energy levels. These three equations describe the bulk density of ions in the fiber at different energy levels in different positions and are the required parameters for the solution of the subsequent power equation, necessary for solving the optical power variation. Equation (4) represents the total ion bulk density, which is the initial condition when designing the fiber, and is a constant in the equation, where the parameters W_{23}, W_{32}, W_P, A_{eff}, σ_{23} ,ν_{23} have the following equations, where the corresponding parameters are shown in Table 1.

$$W_p(z) = \frac{\sigma_{13}(\nu_{13}) \times P_p(z)}{h \times \nu_{13} \times \mathrm{A}_{eff}} \tag{5}$$

$$W_{23}(z) = \frac{\sigma_{23}(\nu_{23}) \times P_s(z)}{h \times \nu_{23} \times \mathrm{A}_{eff}} \tag{6}$$

$$W_p(z) = \frac{\sigma_{32}(\nu_{32}) \times P_s(z)}{h \times \nu_{32} \times \mathrm{A}_{eff}} \tag{7}$$

$$\mathrm{A}_{eff} = \pi \times r^2 \tag{8}$$

$$\sigma_{23}(\nu_{23}) = \sigma_{32}(\nu_{32}) \times \left(\frac{\varepsilon_0 - h \times \nu_{23}}{\kappa \mathrm{T}}\right) \tag{9}$$

$$\varepsilon_0 = h \times \lambda_m \tag{10}$$

2.3 Power transmission equation

For fiber optic systems, the power propagation equation exists as follows:

$$\frac{dP_p(z)}{dz} = \left[-\sigma_p \times N_1(z) - \alpha_p\right] \times P_p(z) \tag{11}$$

$$\frac{dP_s(z)}{dz} = [\sigma_{32} \times N_3(z) - \sigma_{23} \times N_2(z) - \alpha_s] \times P_s(z) \tag{12}$$

$$\frac{dP_{ase}(z)}{dz} = [\sigma_{32} \times N_3(z) - \sigma_{23} \times N_2(z) - \alpha_s] \times P_{ase}(z) + 2 \times \sigma_{32} \times N_3(z) \times h \times \nu_{32} \times \Delta\nu \tag{13}$$

Equation (11) represents the differential equation for the variation of the pump light power with position z in the fiber, where the ground state ions absorb the pump light and the power decreases on the one hand. The power decreases due to the loss attenuation in propagation, on the other hand. Equation (12) represents the differential equation of signal light power with position z. Because the Neodymium ions will absorb the signal light photons in the fiber in $^4I_{15/2}$. And the loss attenuation in the propagation process decreases the signal light power. At the same time, the Neodymium ion cell phone radiation in $^4F_{3/2}$ will also produce the signal light co-channel photons and increase the signal light, when the latter is numerically greater than the former macroscopic performance as the signal light power increases. Equation (13) represents the power of the spontaneously radiated light (ASE light) in the fiber, who is approximately the same frequency as the signal light and also subject to the energy level jump between $^4I_{15/2}$and $^4F_{3/2}$. The attenuation loss of the propagation process, on the basis of which the spontaneous radiation jump of Neodymium ions also increases its power, so to add the last term. The solutions of these three equations are solved by the boundary conditions to obtain the power values of each light at different positions, which is the most direct object of study in this paper. For the calculation of the gain, there is the following equation. The corresponding parameters are shown in Table 1.

$$G_1\left(P_p(z), P_s(z), N_3, N_2, z\right) = \frac{P_s(z)}{P_s(0)}(100\%)L \tag{14}$$

$$G_2\left(P_p(z), P_s(z), N_3, N_2, z\right) = 10 \times \log_{10}\left(\frac{P_s(z)}{P_s(0)}\right)(dB) \tag{15}$$

2.4 Conditions of simulation

The experimental environment of the simulation is assumed to be at room temperature, and the simulation simulates Nd-doped YAG fiber. Due to the short relaxation time, the number of Neodymium ions at each energy level reaches the dynamic equilibrium when reaching the steady state. Then equations (1)-(4) can be written as:

$$W_p(z) \times N_1(z) = A_{21} \times N_2(z) \tag{16}$$

$$W_{23}(z) \times N_2(z) + A_{21} \times N_2(z) = W_{32}(z) \times N_3(z) + A_{32} \times N_3(z) \tag{17}$$

$$W_{32}(z) \times N_3(z) + A_{32} \times N_3(z) = W_p(z) \times N_1(z) + W_{23}(z) \times N_2(z) \tag{18}$$

By solving equations (16)-(18), the volume concentrations of Nd ions at each energy level N1, N2, and N3 at different positions can be obtained, and the absorption cross section of the $^4I_{15/2}$ energy level can be obtained by taking them as equations (9-10).

$$\sigma_{23}(\nu_{23}) = \sigma_{32}(\nu_{32}) \tag{19}$$

The numerical solution of the model can be obtained by bringing the above parameters into the power propagation equation and using the Runge-Kutta methods.

3. Results

3.1 Effect of changed length of fiber-optical

In this experiment, the fiber length is used as the horizontal coordinate for simulation, and the doping concentration of $Nd^{3+\,3+}$ is set to $1.95 \times 10^{24}\, m^{-3}$, the initial power of signal light is $1 \times 10^{-6}\, W$, and the initial power of the pump light is $0.1\, W$. The fiber length is set to L(m), and the signal light gain and optical power obtained by changing the fiber length are shown in Figure 3.

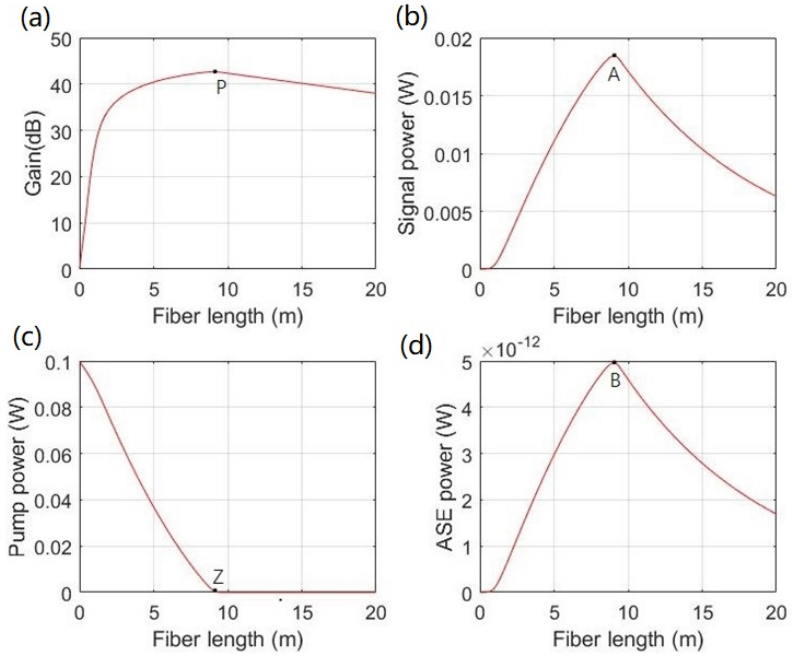


Figure 3. Gain and optical power values for changing doping concentration

As shown in Figure 3(a), the signal optical gain increases with increasing fiber length at $L < 8.92$. The peak point is reached at $L = 8.92$ with a peak value of 42. 65 and a peak point of P. The signal optical gain decreases linearly with increasing fiber length at $L > 8.92$. As in Figures 3(b) and 3(d), the signal optical power and ASE optical power also increase and decrease with the fiber length, and their peaks are at L=8. 92, with peaks of 0. 018W and $4.97 \times 10^{-12} W$, respectively, and the peak points are A, B. As in Figure 3(c), the pump optical power decreases with the increase of L, and decreases to zero at $L = 8.92$, and the zero point is Z, after which it has been. The zero value is

maintained. This is because the Neodymium ions gradually absorb the pump light at the base level as it propagates in the fiber and the power decreases. In this process, the Nd ions at the base level are pumped to the high energy level to form a particle number inversion. The excited radiation of Nd ions at the high energy level increases the optical signal power and ASE optical power. And when the pump light power decreases to 0, the pump light can not maintain the particle number inversion. The optical signal power will be reduced `by loss decay in the transmission process. Therefore, the fiber amplifier should be manufactured so that its length is located at the peak gain. In this simulation, this value is 8.92m.

3.2 Effect of changed doping concentration

$N1$, $N2$, $N3$ represent the doping concentration of Nd^{3+} as $1.5\times10^{24}\,m^{-3}$, $2.0\times10^{24}\,m^{-3}$, $2.5\times10^{24}\,m^{-3}$ respectively. In the fiber length is fixed as $15m$, the initial power of signal light is $1\times10^{-6}W$, the initial power of pump light is $0.1\,W$, and the signal light gain and optical power are obtained by changing the doping concentration images with position coordinate z.

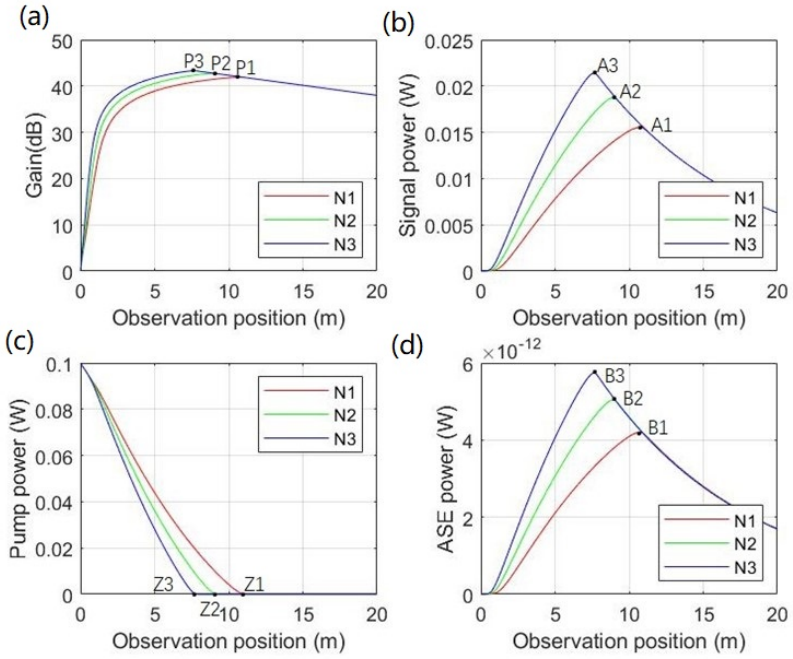


Figure 4. Gain and optical power values for changing doping concentration

As shown in Figure 4(a), when the doping concentration is $N1$, $N2$, $N3$ respectively, the peak signal optical gain arrives at 10. 26m, 8. 90m, 7. 61m and the peaks are 42. 22, 42. 87, 43. 30 corresponding to the points P1, P2, P3 respectively It can be seen that increasing the doping concentration causes the peak to move forward and rise. Then they are parallel but do not overlap in a straight line, as in Figure 5(a). As shown in Figure 4(b), (d), when the doping concentration is $N1$, $N2$, $N3$, the signal optical power reaches the peak at 10. 26m, 8. 90m, 7. 61m with the peak values of 0. 016W, 0. 019W, 0. 021W corresponding to the points A1, A2, A3, respectively. And the ASE signal optical power reaches the peak at 10. 26m, 8. 90m, 7. 61m with the peak values of $4.18\times10^{-12}W$, $5.01\times10^{-12}W$, $5.74\times10^{-12}W$ corresponding to the points B1, B2, B3, respectively. Increasing the doping concentration shifts both their peaks forward and upward. As shown in Figure 4(c), when the doping concentration is $N1$, $N2$, $N3$ respectively, the pump optical power zero points are 10. 26m, 8. 90m, 7. 61m, corresponding to the points Z1, Z2, Z3 respectively. Increasing the doping concentration will make their zero points shift forward.

When the fiber length is $10m$, the initial power of signal light is $0.1uW$, the initial power of pump light is $0.1uW$, the doping concentration varies in the range of $(0.001,\ 3)\times10^{24}m^{-3}$, the fiber amplifier gain variation curve with doping concentration is shown in Figure 5(b). When the doping concentration increases gradually, the gain increases continuously from negative values, and

when $N > 1.78 \times 10^{24}\, m^{-3}$ will reach saturation, and under this condition, the saturation gain value $G = 42.33$. A doping concentration saturation inflection point exists for the optical signal gain of the fiber amplifier. Within the saturation level, the signal gain intensity is sensitive to the doping concentration and can be precisely regulated. Beyond the saturation level, the optical signal gain tends to saturate.

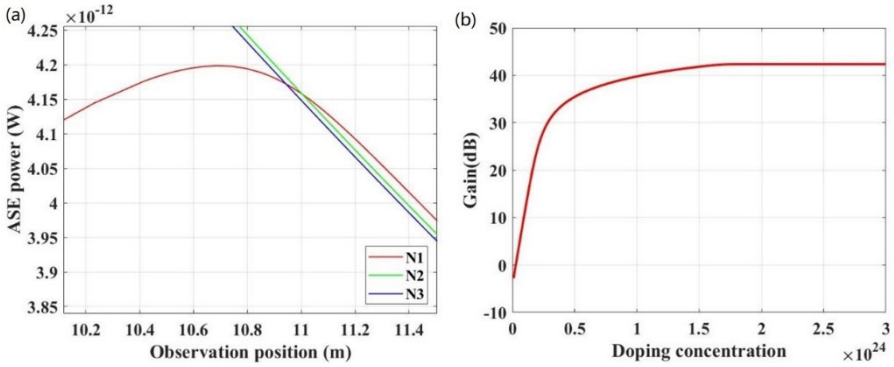


Figure 5.(a) Details of ASE optical power with different doping concentrations.
(b) Image of gain variation with doping concentration

3.3 Effect of changed initial signal optical power

$Ps01$, $Ps02$, $Ps03$ represent the signal light initial optical power of $1 \times 10^{-6}\, W$, $1 \times 10^{-5}\, W$, 1×10^{-4} W, respectively, the fiber length is set to $20\, m$, the Nd^{3+} doping concentration is $1.95 \times 1024\, m^{-3}$, the initial pump power is $0.1W$, and the gain and optical power of the initial signal optical power are varied to obtain the signal The images of optical gain and optical power with position coordinate z were obtained.

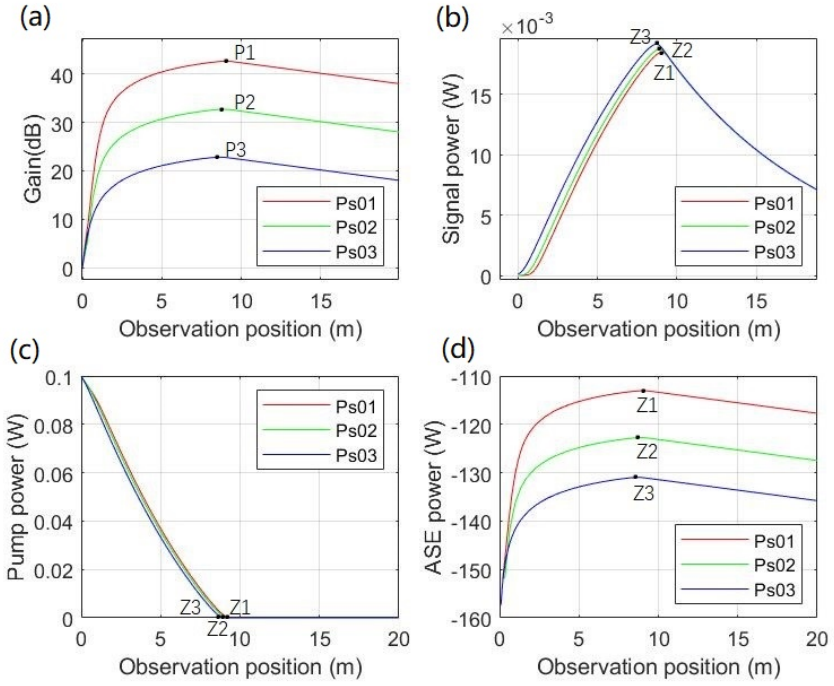


Figure 6. Gain and optical power values for changing the initial power of the signal light.

As shown in Figure 6(a), when the initial signal light power is $Ps01$, $Ps02$, $Ps03$ respectively, the peak signal light gain arrives at 8. 62m, 8. 73m, 8. 78m, and the peaks are 42. 63, 32. 70, 22. 81 corresponding to points P1, P2, P3 respectively. it can be seen that the initial signal light power increases will make the peaks move forward and fall, and then they are The partial parallel but not coincident straight line decreases. As in Figure 6(b), when the initial power of signal light is $Ps01$,

$Ps02$, $Ps03$, respectively, the signal light power reaches the peak positions of 8. 62m, 8. 73m, 8. 78m, and the peaks are 0. 0186W, 0. 0187W, 0. 191W corresponding to the points A1, A2, A3, respectively, and it can be seen that their subsequent linear descents partially overlap, as in Figure 7(b). As in Figure 6(c), when the initial signal light power is $Ps01$, $Ps02$, $Ps03$, the pump light power zero points are 8. 62m, 8. 73m, 8. 78m, corresponding to the points Z1, Z2, Z3, respectively, the initial signal light power increases will make their zero points move forward. The details are shown in Figure 7(a). The ASE signal optical power is taken as the logarithm as the vertical coordinate, and the positions where it reaches the peak are 8. 62m, 8. 73m, 8. 78m, and the peak power values are 5. 01×10^{-13}W, 5. 38×10^{-14}W, 8. 08×10^{-15}W corresponding to points B1, B2, B3 respectively. It can be seen that the initial signal optical power increase will make their peaks both forward and down, and then they are parallel but do not overlap in a straight line down part, as in Figure 6(d).

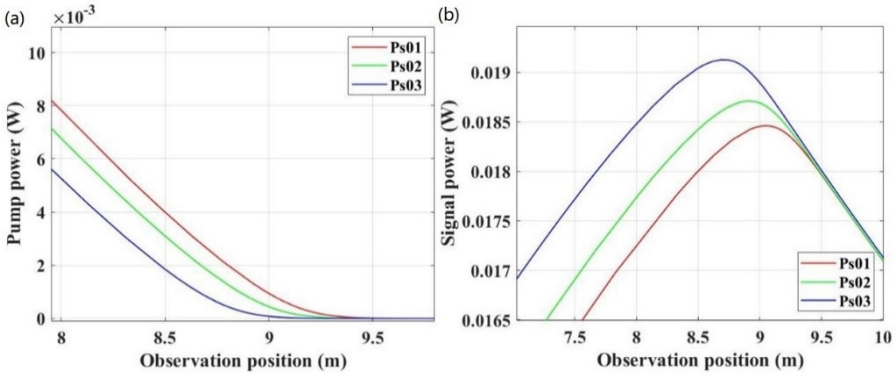


Figure 7. (a) Details of pump optical power for different signal optical power initial values. (b) Details of the peak signal optical power for different signal optical power initial values

When the fiber length is $10m$, the doping concentration is $1.95 \times 10^{24}\ m^{-3}$, the initial power of pump light is $0.1W$, and the initial power of signal light varies in the range of $(0.0001,\ 1) \times 10^{-3}W$. The fiber amplifier gain variation curve with the initial power of signal light is shown in Figure 8(a).

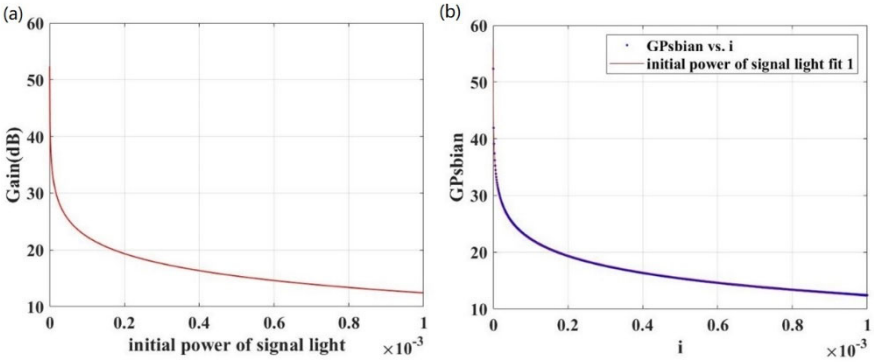


Figure 8. (a) Image of gain variation with initial power of signal light.(b) Fitted data relationship diagram

It can be seen that the fiber amplifier gain gradually decreases as the initial power of the signal light increases. The fitted curve and the original data relationship obtained by fitting the above curve are shown in Figure 8(b), with a goodness-of-fit of 0. 9983, which can be used for data estimation. The fitted functional expression is as follows.

$$G = 29.1372 \times (Ps0)^{-0..0688} \times e^{-31.29\times(Ps0)^{0.9312}} - 32.38 \qquad (20)$$

The signal light gain of the fiber optic amplifier decreases as the initial power of the signal light increases, and it decreases more and more slowly. Therefore, low power signal light can achieve a large gain amplification, and high power signal light can be precisely regulated signal light gain.

3.4 Effect of changed initial pump power

$Pp01$，$Pp02$，$Pp03$ represent the initial pump light power of $0.1\,W$, $0.15\,W$, $0.2\,W$ fiber length is set to 20 m, Nd^{3+}doping concentration is $1.95\times10^{24}\,m^{-3}$, change the initial pump light power gain and optical power to obtain the signal optical gain and optical power with position coordinate z.

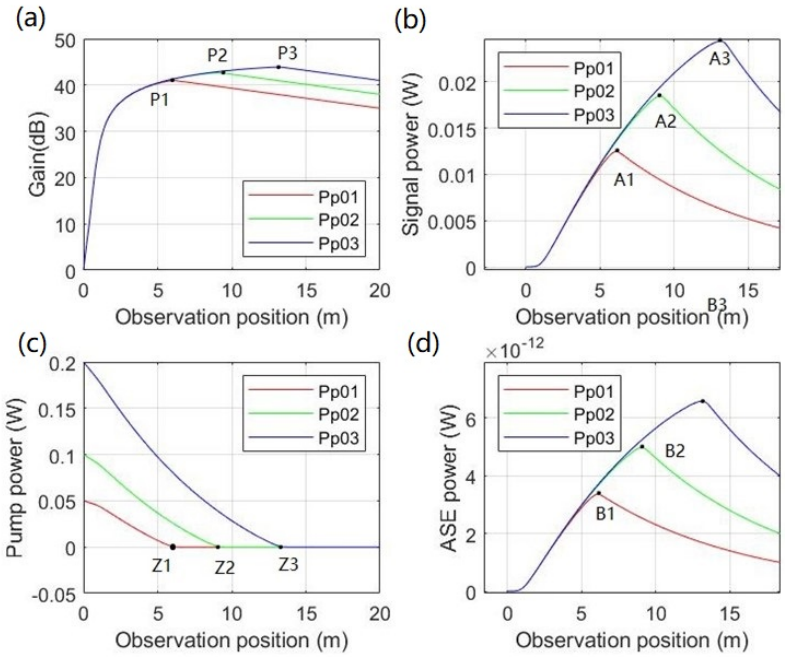


Figure 9. Gain of the initial power for changing the pump light with the value of optical power

As in Figure 9(a), when the initial pump optical power is $Pp01$，$Pp02$ and $Pp03$, respectively, the signal optical gain peak arrival positions are 6. 05m, 9. 31m, and 13. 14m, and the peaks are 40. 95, 42. 99, and 43. 87, corresponding to points P1, P2, and P3, respectively. The increased doping concentration causes the peak to move back and up and the images of the three pump powers coincide completely before reaching the peak. Then they are parallel but not coincident in the part of the linear decline. As in Figure 9(b), (d), when the initial pump optical power is $Pp01$，$Pp02$，$Pp03$ respectively, the optical signal power reaches the peak positions of 6. 05m, 9. 31m, 13. 14m, and the peaks are 0. 12W, 0. 18W, 0. 24W corresponding to points A1, A2, A3 respectively. The locations where the ASE signal optical power reaches its peak are 6. 05m, 9. 31m, and 13. 14m, and the peaks are 3. 49×10^{-12}W, 5. 12×10^{-12}W, and 6. 57×10^{-12}W corresponds to points B1, B2, and B3, respectively. An increase in doping concentration shifts their peaks both backward and upward. As shown in Figure 9(c), when the initial pump optical power is $Pp01$，$Pp02$，$Pp03$, the pump optical power zero points are 6. 05m, 9. 31m, 13. 14m, respectively, corresponding to the points Z1, Z2, Z3 can be seen that increasing the doping concentration will make their zero points shift back.

When the fiber length is $10m$, the doping concentration is $1.95\times10^{24}\,m^{-3}$, the initial power of signal light is $0.1uW$, and the initial power of pump light varies in the range of $(0.0001,\ 0.2)m^{-3}$, the fiber amplifier gain variation curve with the initial power of pump light is shown in Figure 10(a).

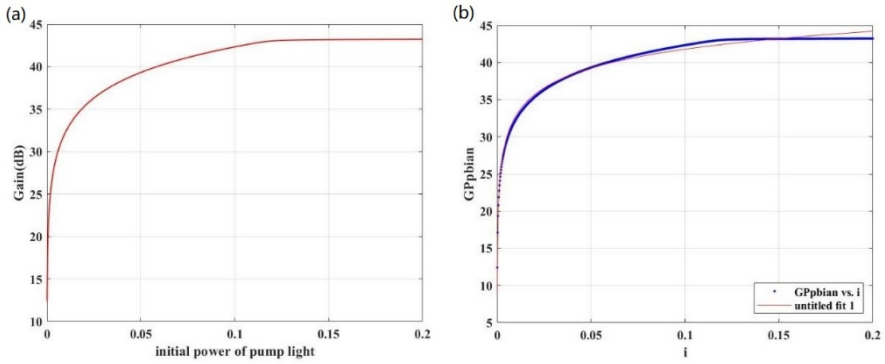


Figure 10. (a) Gain variation with pump light initial power.(b) Fitted data relationship diagram

With the increase of the pump light's initial power, the fiber amplifier's gain increases continuously and reaches the saturation state when $Pp0 > 0.15W$, and the value of its saturation state $G = 43.19$. The fitted curve of the above curve and the original data are shown in Figure 10(b). The goodness-of-fit is 0. 987, which can be approximated at $Pp < 0.14$, and the expression of the fitting function is as follows

$$G = -39.23 \times (Pp0)^{-0.07629} + 88.55 \quad (21)$$

For the optical signal gain of the fiber amplifier there exists a doped initial pump light power saturation inflection point. The signal optical gain intensity is sensitive to the initial pump light power and can be precisely regulated within the saturation degree. Beyond saturation, the optical signal gain tends to saturate.

3.5 Explorations of the asymptotic line

There is a linear asymptote in the image of the power variation with position z in the fiber and in the finding that the slope of the line does not vary with the four parameters studied in this paper and is constant in this numerical simulation. The constant term of the linear expression is only related to the signal light's initial power and the pump light's initial power. It is independent of both the doping concentration and the fiber length. Therefore, asymptotic experiments are performed to prove this law's existence numerically and obtain a fitting expression for this asymptotic line. It can be useful for theoretical studies in optical fibers and easy estimation of the gain of Nd-doped optical fiber amplifiers for applications, as shown in Figure 11 below.

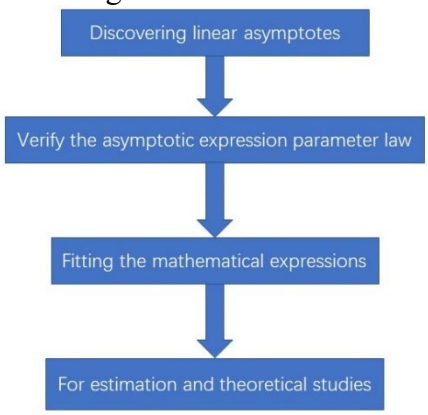


Figure 11. Logic Flow Chart

From the above analysis, the signal optical power gain of the fiber amplifier exists only with the initial signal optical power, the initial pump optical power related to the linear shape asymptote. The concentration only affects the distance z required to reach this asymptote, and the maximum gain of the amplifier are also in this asymptote, set the asymptote linear expression as follows.

$$G = K \times z + B \tag{22}$$

Therefore, the initial pump power is$0.1W$, the $\boldsymbol{Nd^{3+}}$ doping concentration is $1.95 \times 1024\, m^{-3}$, and the fiber length is $20m$. The initial value of the signal light is taken from $1 \times 10^{-7}W$ to $1 \times 10^{-3}W$ with an interval of $1 \times 10^{-6}W$. A total of 1000 sets of data are taken, and their numerical solutions for the gain variation with length are calculated separately. Then, the least-squares regression is performed on the approximately linear part of each solution to find the relationship between its asymptotic expression and the initial value of the optical signal power. Figures 29-30 show the graphs of the slope K and the ensemble superiority R_2 with the initial value of the optical signal power, respectively. The goodness of fit is greater than 0. 999. So in the peak gain $z0$ and $z > z0$ part of the fiber amplifier gain and signal initial optical power is linear. The slope are around 0. 43 and the initial value of the optical signal power in the (1 × 10-4W, 1 × 10-6W) range is constant. Using its expectation estimate K, can be derived $K = -0.433W^{-1}$. Figure 16 shows the image of the variation of the constant B with the initial value of the optical signal power.

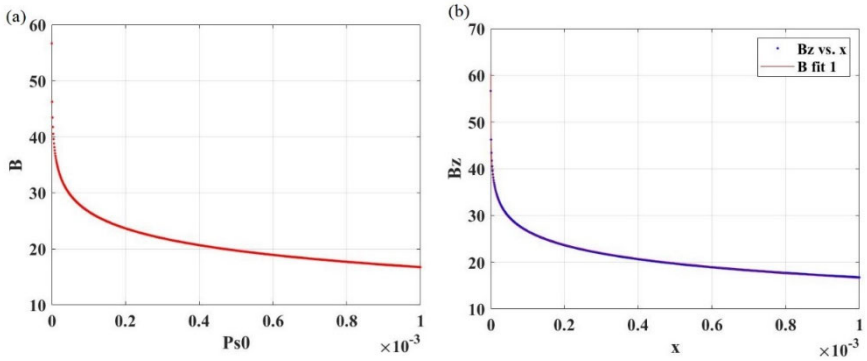


Figure 12. (a) Scatter plot of B with the initial value of optical power of different signals. (b) Fitted data relationship diagram

The image of this constant term B can be fitted to obtain B in line with the Weber distribution curve based on adding a constant. The fit results are shown in Figure 17, the goodness of fit is 0. 9983. The functional expression of $G$is as follows

$$B = a \times b \times (Ps0)^{b-1} \times e^{-a \times (Ps0)^b} + c \tag{23}$$

In the data of this experiment$a = 33.17$，$b = 0.9312$，$c = -28.03$

And on the basis of this further change the value of pump power, where the pump light initial power from 0. 002 to 0. 2 taken a total of 100 groups, the goodness of fit of these 100 groups is shown in Figure 13(a). Except for the 10 data with low goodness of fit at the beginning and a few data with low goodness of fit in the middle, the goodness of fit of the rest of the data was greater than 0. 997. Then the values of a, b, and c are plotted against the initial power of the pump light in Figure 13(b), (c), and (d), respectively.

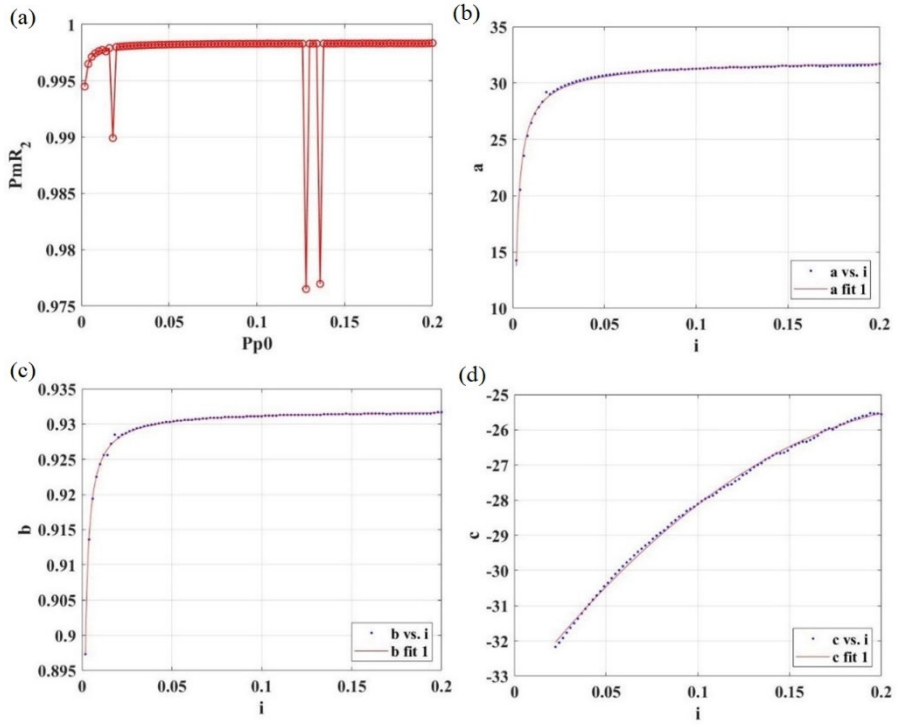


Figure 13. Goodness of fit with parameters a, b, c images

where the goodness of fit of parameters a, b, and c reaches 0. 9963, 0. 9989, and 0. 9989, and the obtained expressions for a, b, and c are as follows:

$$a = -0.203 \times (Pp0)^{-0.7269} + 32.35 \quad (24)$$

$$b = -1.102 \times 10^{-4} \times (Pp0)^{-0.9268} + 0.9321 \quad (25)$$

$$c = -184.5 + 151.1 \times \cos(-1.329 \times Pp0) - 50.44 \times \sin(-1.329 \times Pp0) \quad (26)$$

The asymptotic expressions are as follows:

$$G = K \times z + B \quad (22)$$

In the above equation $K = -0.4315W^{-1}$ and B can be determined by equations (23)-(26). The initial value of pump optical power to fiber amplifier gain is exponential, and the signal light to fiber amplifier gain is a Weber distribution function. It has the same form as the results obtained in equations (20-21) for the two fixed variables of 3. 3 and 3. 4.

4. Conclusions

In this paper, a mathematical model of a Neodymium-doped fiber amplifier is established, and the relationship between its gain, optical power, and the four independent variables studied in this paper is summarized. At the same time, the asymptote of its gain is found and the mathematical expression of the asymptote is given by numerical fitting. The gain of the Nd^{3+} doped fiber amplifier can be obtained from the experiments as its length increases, decreasing first and then increasing, with a peak gain. The gain of the amplifier increases with its doping concentration, and the rate becomes slower and slower and finally saturates, which may be since the concentration reaches the limit of the absorption of the pumped light. Too many Nd ions cannot be pumped to higher energy levels. The amplifier gain gradually decreases with the increase of its signal light initial power, and the amplifier gain increases with the rise of its pump light power and finally tends to saturate, which may be due to the fact that the particle number inversion tends to the limit and the majority of particles are already at high energy levels. During this numerical simulation, the amplifier's peak gain and the length after the peak decrease linearly. And there is a linear shape of the asymptote. The slope of this asymptote is independent of the four parameters studied above. The constant term in the linear expression is only related to the signal light's initial power and the pump light's initial power, based on which the experimental data results are fitted numerically to obtain its calculated expression. However, in this

experiment, only the expression given does not have a theoretical explanation, which can be further studied.

References

[1] Zhao Gan. Study of fiber optic loss in engineering practice [D]. Shandong University, 2010.

[2] Grassi, F. et al., 2010. Radio over fiber transceiver employing phase modulation of an optical broadband source. Optics Express, 18(21), p.21750.

[3] Wang Daizhi, Li Chao. Research on improving the shooting accuracy of laser end-guided weapon system in battlefield countermeasure environment [J]. Ship Electronic Engineering, 2022, 42(04):171-175+180.

[4] Zhang Anjun, Duan Jialin, Xing Yingbin, Li Jinyan. Thulium-doped laser in the biomedical field [J]. Laser & Optoelectronics Progress, 2022, 59(01):50-63.

[5] Mei Fa. Study on radiation attenuation of erbium-doped fiber for laser communication terminal under space irradiation [D]. Harbin Institute of Technology, 2021. DOI:10. 27061/d. cnki. ghgdu. 2021. 003991.

[6] Mingareev, I. et al., 2012. Welding of polymers using a 2MM thulium fiber laser. Optics & Laser Technology, 44(7), pp.2095–2099.

[7] Bashkatov, A.N., 2005. Optical properties of the subcutaneous adipose tissue in the spectral range 400–2500 nm. Optics and Spectroscopy, 99(5), p.836.

[8] Agger, S., Povlsen, J.H. & Varming, P., 2004. Single-frequency thulium-doped distributed-feedback fiber laser. Optics Letters, 29(13), p.1503.

[9] Quimby, R.S. et al., 2008. Modeling of cascade lasing in dy : Chalcogenide glass fiber laser with efficient output at 4.5 μm. IEEE Photonics Technology Letters, 20(2), pp.123–125.

[10] Quimby, R.S. & Saad, M., 2013. Dy:fluoroindate fiber laser at 4.5 μm with Cascade Lasing. Advanced Solid-State Lasers Congress.

[11] Daniel, J.M. et al., 2014. Ultra-short wavelength operation of a two-micron thulium fiber laser. CLEO: 2014.

[12] Zhang, Y. et al., 2019. Tunable Random Raman fiber laser at 1.7 μm region with high spectral purity. 2019 18th International Conference on Optical Communications and Networks (ICOCN).

[13] Chen, S. et al., 2020. All-fiber short-wavelength tunable mode-locked fiber laser using normal dispersion thulium-doped fiber. Optics Express, 28(12), p.17570.

[14] Chen, J.-X. et al., 2021. 1.7-μm dissipative soliton TM-doped Fiber Laser. Photonics Research, 9(5), p.873.

[15] Grimes, A.T., Hariharan, A. & Nicholson, J.W., 2021. Progress on high power Raman fiber lasers at 1.48 and 1.7 μm. Fiber Lasers XVIII: Technology and Systems.

[16] Zhu Yihuai, Shen Pengsheng, Zheng Shukai, Yu Linpeng, Luo Xing, Wang Jinzhang, Yan Peiguang, Lv Qitao, Dong Fanlong, Guo Chunyu, Ruan Shuangchen 1. 7μm self-synchronized picosecond pulsed random Raman fiber laser [J]. Journal of Shenzhen University(Science & Engineering), 2022, 39(04):363-368.

[17] Wang Yi. Characterization of a new all-solid-state human-eye safe neodymium-doped laser based on ~4F_(3/2)→~4I_(15/2) leap [D]. Xiamen University, 2017.

[18] M. Pokhrel, N. Ray, G. A. Kumar, D. K. Sardar. Comparative studies of the spectroscopic properties of Nd3+: YAG nanocrystals, transparent ceramic and single crystal[J]. Optical Materials Express, 2012, 2(3).

[19] Gan Fuxi, Chen Shuchun, Hu Hefang. Radiation-free energy transfer process in Nd-doped laser glass [J]. SCIENTIA SINICA, 1981(03):289-295.

[20] Gan Fuxi. Energy transfer process of neodymium ion Nd~(3+) in inorganic glass II . Radiation-free leap [J]. Chinese Science Bulletin, 1979(02):59-62.